Journal of Functional Foods 94 (2022) 105118

Contents lists available at ScienceDirect

Journal of Functional Foods

journal homepage: www.elsevier.com/locate/jff

EGCG regulated osteolytic microenvironment to enhance the antitumor effect of DOX on orthotopic osteosarcoma

Dongcai Hu [a], KeJiang Lin [c], Xiang Gao [a], Mengxue Zhou [b,*], Huan Geng [a,*]

[a] Department of Orthopedics, The Second Affiliated Hospital, School of Medicine, Zhejiang University, Hangzhou, China
[b] Key Laboratory of Tea Biology and Resource Utilization of Ministry of Agriculture, Tea Research Institute, Chinese Academy of Agricultural Sciences, Hangzhou 310008, China
[c] Hospital of Traditional Chinese Medicine of Yushan Affiliated to Jiangxi University of Traditional Chinese Medicine, Shangrao 334700, China

ARTICLE INFO

Keywords:
Orthotopic osteosarcoma
Osteolysis
EGCG
Doxorubicin
Chemotherapy

ABSTRACT

Osteosarcoma is the most common malignant bone tumor with the pathological essence of osteolysis. Doxorubicin (DOX) is common in adjuvant chemotherapy of osteosarcoma. However, it is required to address the conflict between enhancing its dose to improve efficacy and reducing its complications and chemotherapy resistance. Previous studies have demonstrated that EGCG has an antitumor and osteoclastogenesis inhibition effect. However, the combined effect of EGCG and DOX on osteosarcoma is still unclear. Here, EGCG was demonstrated to enhance the 143B cell proliferation inhibition and anti-osteoclastogenesis effect of DOX in vitro. The results suggest that EGCG in synergy with DOX inhibited AKT phosphorylation, which was involved in 143B cells proliferation and osteoclastogenesis. In vivo, the combination of DOX and EGCG could reduce tumor volume and osteolysis destruction compared with the DOX treatment group. This present study raised the possibility that EGCG may be used as an adjuvant chemotherapy drug to treat osteosarcoma.

1. Introduction

Osteosarcoma is the most common primary bone malignancy in children and adolescents (Du et al., 2021; Geng et al., 2021). Although with the treatment of neoadjuvant chemotherapy and surgical resection, the overall 5-year survival rate for osteosarcoma patients attains 65–70%, the survival rate for those with chemotherapy resistance or metastasis is only 15–30% (Gill & Gorlick, 2021).

Doxorubicin (DOX) is one of the classical chemotherapeutic drugs for osteosarcoma (Baa & Rastogi, 2021; Ruan et al., 2022; Zhou et al., 2019). However, the intrinsic weakness of DOX undermines the efficacy of this treatment clinically: low-dose usage could not only attenuate its effectiveness but also lead to chemoresistance; at the same time, dose increase is related to serious side effects (Wang, Chen, & Zhu, 2018). At present, three-drug chemotherapy regimens can partially improve the effect on killing osteosarcoma cells, such as methotrexate, doxorubicin (adriamycin) and cisplatin (platinol) (Liu, Geng, Mei, & Chen, 2021). However, there is no combined strategy for osteosarcoma that can significantly improve the efficacy and undermine these side effects of these drugs. Therefore, a novel and more effective treatment with lower side effects is needed to complement the current strategy to improve overall survival.

Osteolysis is a common manifestation of osteosarcoma, even within predominantly osteoblastic lesions, and is mediated by osteoclasts and their bone-resorbing activity (Labrinidis et al., 2009). Osteoclasts play a crucial role during the tumor-induced osteolytic process. Osteoclast progenitors express RANK receptors, while osteosarcoma cells can produce a large number of RANK ligands (RANKLs) that promote osteoclast

Abbreviations: EGCG, epigallocatechin gallate; DOX, doxorubicin; BMMs, bone marrow-derived macrophages; M-CSF, macrophage colony-stimulating factor; RANK, receptor activator of NF-κB; RANKL, Receptor activator of NF-κB ligand; H&E, hematoxylin and eosin; AKT, protein kinase B; GAPDH, glyceraldehyde-phosphate dehydrogenase; TRAP, tartrate-resistant acid phosphatase; CDI, coefficient of drug interaction; CCK-8, cell counting kit 8; SDS-PAGE, sodium dodecyl sulfate-polyacrylamide gel electrophoresis; OD, optical density; DAPI, 4′,6-diamidino-2-phenylindole; α-MEM, alpha-minimum essential medium; MOD, mean optical density; FBS, fetal bovine serum; RIPA, radioimmunoprecipitation assay; Micro-CT, micro-computed tomography; BMD, bone mineral density; BV/TV, trabecular bone volume per tissue volume; Tb. N, trabecular number; Tb. Th, trabecular thickness; Tb. Sp, trabecular separation; EDTA, ethylene diamine tetraacetic acid; HRP, horseradish peroxidase; SPSS, statistical product service solutions; ANOVA, analysis of variance; SD, standard deviation.

* Corresponding authors.
E-mail addresses: zhoumengxue@tricaas.com (M. Zhou), genghuan1989@zju.edu.cn (H. Geng).

https://doi.org/10.1016/j.jff.2022.105118
Received 30 March 2022; Received in revised form 14 May 2022; Accepted 16 May 2022
Available online 19 May 2022

differentiation and activity (Geng et al., 2017). In turn, osteoclasts resorbed bone matrix and released a variety of factors that favor osteosarcoma growth. These accelerating events are often termed a "vicious circle" (Lee et al., 2011). Thus, osteoclasts targeted therapy is a potential treatment for osteosarcoma, and some osteoclast-targeting drugs have inhibited tumors effectively (Chen et al., 2015). Epigallocatechin gallate (EGCG) is the major catechin in green tea with many physiological and pharmacological activities (Gan, Li, Sui, & Corke, 2018). Moreover, various studies have shown that EGCG can inhibit osteoclast differentiation (Xu et al., 2021; Xu et al., 2019). However, whether EGCG combining DOX can enhance the inhibition of osteosarcoma growth remains unclear.

In this study, we examined the efficacy of combined therapy with DOX and EGCG on osteosarcoma. We demonstrated that the combination of EGCG and DOX could produce a synergistic effect on osteosarcoma cell growth inhibition and osteoclast formation. The mechanism of synergistic effect was mainly related to AKT inactivation, which plays a crucial role in cell proliferation and osteoclastogenesis. Furthermore, we confirmed the synergistic antitumor effect of combined treatment with EGCG and DOX in mouse-bearing orthotopic osteosarcoma, and it inhibited bone destruction by substantially attenuating osteoclast activity, which prevented the formation of the aforementioned vicious circle.

2. Materials and methods

2.1. Cell viability assay

The viability of the 143B cells was assessed by a CCK-8 assay. The cells were seeded in 96-well plates (5000 cells in 100 mL medium). After incubating for 24 h, the 143B cells was incubated with DOX (0, 0.5 μg/mL) and EGCG (0, 15 μg/mL) for 0, 24 or 48 h. At predetermined time intervals, the cells were washed with PBS. Then fresh medium containing 10% CCK-8 was added to each well and incubated at 37 °C for 30 min. The UV–vis absorbance was measured using a microplate reader (SpectraMax M5, Molecular Devices, Sunnyvale, CA, USA) at 450 nm. Cell proliferation inhibition ratio (%) was calculated according to the absorbance (OD). Cell proliferation inhibition ratio (%) = (OD value of control group – OD value of treated group)/OD value of control group × 100%. The coefficient of drug interaction (CDI) = AB / (A × B). According to the OD value of each group, AB is the OD value of the combination groups to the control group; A or B is the OD value of the single-agent group to the control group. Thus, synergistic effect: CDI < 1, additive effect: CDI = 1, antagonistic effect: CDI > 1, respectively.

2.2. Colony formation assays

For colony formation assay, the 143B cells (1000 cells/well) were seeded in 6-well plates and allowed to culture for 24 h. Once the cells were fully attached to the wall, the cells were incubated with 0.5 μg/mL DOX or 15 μg/mL EGCG. After 7 days, the cell colonies were fixed with 4% paraformaldehyde and stained with crystal violet. The cells were photographed and the number of colonies (>50 cells) was counted. Clone formation rate (%) = (Clone number of control group – Clone number of treated group) / Clone number of control group × 100%.

2.3. Immunofluorescence staining

The Ki-67 immunofluorescence analysis was exploited to evaluate cell proliferation. The 143B cells (5×10^4 cells/dish) were seeded in confocal dishes for 24 h and then incubated with 0.5 μg/mL DOX or 15 μg/mL EGCG for 48 h. Then the cells were washed twice with PBS, fixed in 4% paraformaldehyde for 20 min, and permeated in 0.1% Triton X-100 for 15 min at room temperature. The cells were then treated with a blocking buffer and incubated with primary antibodies against Ki-67 at 4 °C overnight. Subsequently, the cells were incubated with a secondary antibody at room temperature for 1 h. Cell nuclei were stained with DAPI, and fluorescence images were acquired using confocal laser scanning microscopy (Nikon Ti-E imaging system, Tokyo, Japan). ImageJ software (National Institutes of Health, Bethesda, MD, USA) was used for quantitative analysis.

2.4. Formation of osteoclast cells in vitro

Primary bone marrow cells were isolated from 4-week-old BALB/c mice euthanized by cervical dislocation and cultured in a complete medium (α-MEM containing 10% fetal bovine serum [FBS], 1% penicillin, and 1% streptomycin) supplemented with 50 ng/mL M-CSF for 3 days to obtain bone marrow-derived macrophages (BMMs). For osteoclastogenesis, BMMs were seeded in 96-well plates (1×10^4 cells/well) and cultured in a complete medium supplemented with 50 ng/mL M-CSF and 50 ng/mL RANKL for 4 days to generate mature osteoclasts. The complete culture medium containing different supplements was renewed every 2 days and 0.5 μg/mL DOX or 15 μg/mL EGCG was added. The cells were fixed with 4% paraformaldehyde and stained using the TRAP staining kit according to the manufacturers' instructions. The $TRAP^+$ multinucleated (>3 nuclei) cells were counted as osteoclasts.

2.5. Bone resorption assay

BMMs (2×10^4 cells/well) were cultured in Osteo Assay Surface 24-well plates (Corning, NY, USA), which were coated with a calcium phosphate substrate. After 24 h, the medium was removed, and a complete inducing medium with 0.5 μg/mL DOX or 15 μg/mL EGCG was added. The culture medium was replaced every 2 days. After 6 days of culture, the cells were washed with 10% sodium hypochlorite and rinsed with water three times. The images were captured using an ordinary light microscope after the cells were completely dried at room temperature. The percentage of the resorbed bone surface area was quantified by using ImageJ software.

2.6. Western blotting

Cells were washed twice with PBS and lysed in ice-cold RIPA Lysis Buffer (Beyotime, China) containing protease inhibitors (Beyotime, China), incubated on ice for 20 min to extract total protein, and centrifuged at 4 °C at 12,000 g. An equal amount of protein (50 μg) from each sample was mixed with sodium dodecyl sulphate-polyacrylamide gel electrophoresis (SDS-PAGE) loading buffer (Beyotime, China) and then heated at 95 °C for 5 min. Subsequently, protein lysates were resolved by SDS-PAGE on 12 % polyacrylamide gels, transferred to polyvinylidene difluoride membranes, and blotted with specific primary antibodies against AKT and p-AKT (Cell Signaling Technology, Danvers, MA) overnight at 4 °C. Band intensity was quantified by using Quantity One (Bio-Rad, Shanghai, China).

2.7. Animals and treatment

All animal care was approved by the Animal Welfare Committee in Zhejiang University School of Medicine (Permit Number: 2020–0011). 4–6 week-old male BALB/c nude mice were purchased from Beijing Vital River Laboratory Animal Technology Co., Ltd. (NO.2103241913023172). Orthotopic tumor models can better simulate the growth state of tumors in vivo (Ren et al., 2021). To construct an orthotopic osteosarcoma mouse model, the 143B cells suspension (5×10^5) in 10 μL PBS was injected into the proximal right tibia in nude mice using a 25-gauge needle after anesthetized. 7 days after the inoculation, the mice were randomly divided into 4 groups with 4 mice in each group: (a) Saline, (b) DOX (5 mg/kg), (c) DOX + EGCG (5 mg/kg DOX + 30 mg/kg EGCG), 4 normal nude mice without the tumor cell inoculation were regarded as a control group. The above reagents were injected

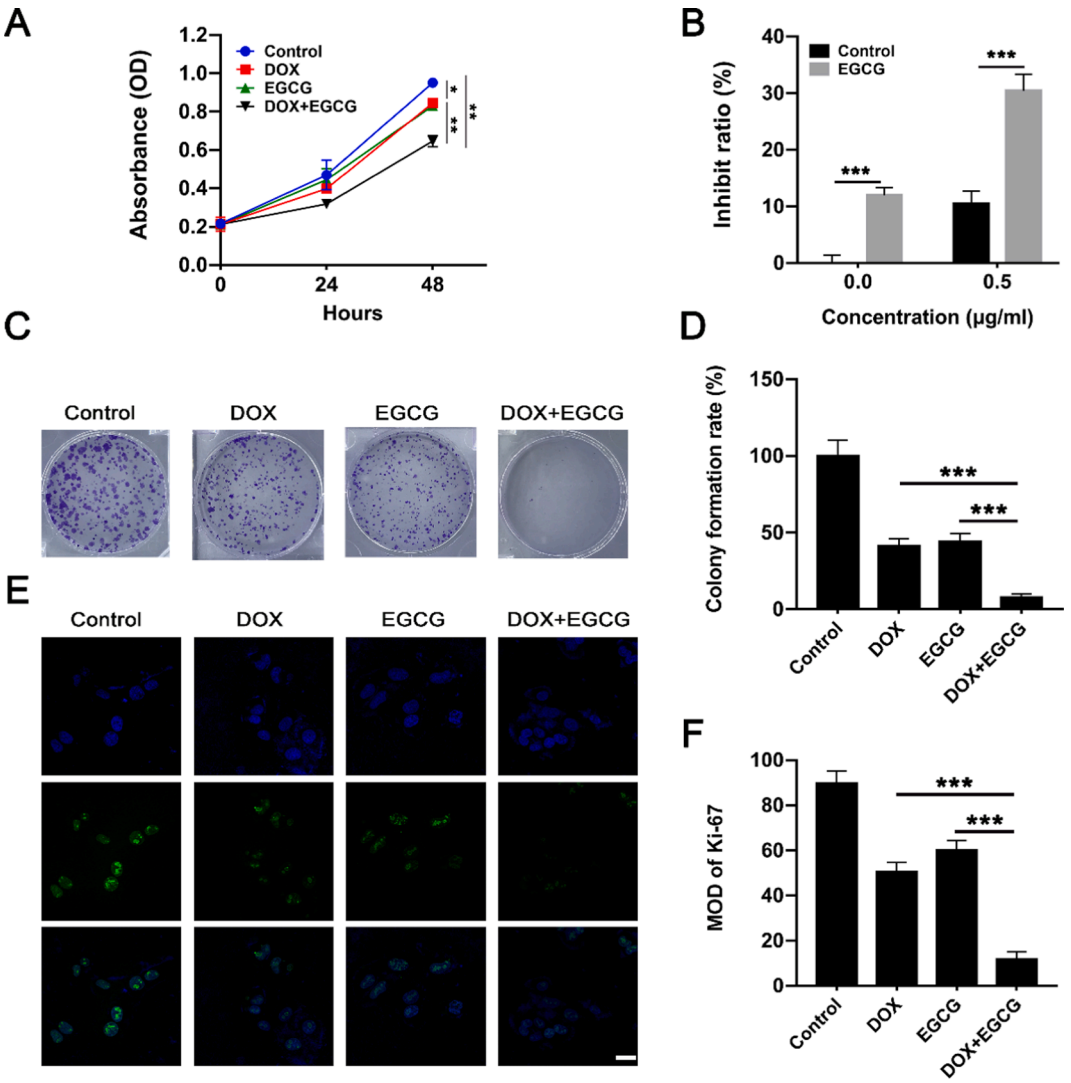

Fig. 1. EGCG increased DOX-induced proliferation inhibition in 143B cells. (A) CCK-8 assay evaluated the viability of 143B cells treated with DOX/EGCG/combination for 0, 24 and 48 h, respectively. (B) The combination of EGCG and DOX synergistically facilitates antitumor effects in 143B cells. (C) Cell clone formation of the 143B cells treated with DOX/EGCG/combination. (D) The clone formation rate of the 143B cells under different treatments. (E) Confocal analysis was used to detect Ki-67 protein expression in 143B cells treated with DOX/EGCG/combination (Nucleus is in blue and Ki-67 is in green). Scale bar = 25 μm. (F) The Ki-67 expression was quantified by the MOD value. Data are mean ± SD of triplicate experiments, $*P < 0.05$, $**P < 0.01$, $***P < 0.001$. (For interpretation of the references to colour in this figure legend, the reader is referred to the web version of this article.)

intraperitoneally 5 times once every 3 days. The body weight and tumor growth were measured every other day. Tumor volume was calculated by the following formula: volume = (length × width^2)/2. Finally, all mice were sacrificed and the tumor of each mouse was collected for further analysis. The tumor with the tibia was weighed after the excision.

2.8. Micro-computed tomography analysis

After the animal was sacrificed, the tumor of each mouse as well as the major organs, including heart, liver, spleen, lung and kidney, were collected for further evaluation. All the samples of the tumor-bearing left tibias were fixed in 4% paraformaldehyde while the right femurs were fixed in 75% ethanol. All the samples of the tumor-bearing left tibias were scanned with a micro-CT (Quantum GX, PerkinElmer) immediately after the chemical fixation. A three-dimensional reconstruction image for each tumor-bearing tibia was acquired. The bone parameters, including bone mineral density (BMD), trabecular bone volume per tissue volume (BV/TV), trabecular number (Tb. N), trabecular thickness (Tb. Th) and trabecular separation (Tb. Sp) of the scanned right femurs were analyzed by using the software (Analyze 12.0, PerkinElmer).

2.9. Histochemistry, immunohistochemistry and histomorphometric analysis

The tumor-bearing left tibias were fixed in 4% paraformaldehyde for 48 h, decalcified in 0.5 M EDTA for 4 weeks and embedded in paraffin. After being fixed in 4% paraformaldehyde for 48 h, the heart, liver, spleen, lung and kidney were embedded in paraffin directly. Five-micrometers-thick sections of all samples were processed for hematoxylin and eosin (H&E) staining. Sections of the tumor-bearing tibias, the right tibias and the calvarias were performed TRAP staining using the standard protocol. Immunostaining was also performed using the standard protocol. After antigen retrieval, sections of tumor-bearing tibias were incubated with primary antibodies to Ki-67 (dilution 1:800), respectively. Subsequently, an HRP-streptavidin detection system was used to measure the immunoactivity and then counterstained with hematoxylin was followed (Sigma-Aldrich). The luminescence microscopical images of the slices were obtained with an inverted luminescence microscope (Olympus X-73, Japan).

Table 1
Dosage inhibitory effects of both EGCG and DOX on the cells (n = 3).

Drug	Concentration	Growth inhibitory effects (OD value)	CDI
DOX	0 μg/mL	0.951 ± 0.014	–
	0.5 μg/mL	0.846 ± 0.022	–
DOX + EGCG	0 μg/mL + 15 μg/mL	0.831 ± 0.013	–
	0.5 μg/mL + 15 μg/mL	0.647 ± 0.029	0.921 ± 0.035

CDI was measured as described in materials and methods with DOX, EGCG or both agents for 48 h. Synergistic effect: CDI < 1; Additive effect: CDI = 1; Antagonistic effect: CDI > 1.

2.10. Statistical analysis

Statistical analysis was performed using SPSS ver. 20.0 software (IBM Corp, Armonk, NY, USA). Data are represented as mean ± SD. Statistical differences were assessed by one-way analysis of variance (ANOVA) and $P < 0.05$ was considered a statistically significant difference.

3. Results

3.1. EGCG enhanced DOX-induced proliferation inhibition of 143B cells

Firstly, Cell Counting Kit 8 (CCK-8) assay was used to determine whether EGCG could produce synergistic effects with DOX on 143B cells proliferation inhibition. The coefficient of drug interaction (CDI) was calculated. The results showed that the proliferation inhibition was significantly upregulated when DOX was used in combination with EGCG (Fig. 1A and B). As expected, according to the CCK-8 assay and the coefficient of drug interaction (CDI, shown in Table1), EGCG and DOX yielded synergistic interactions (CDI < 1). Cell clone and immunofluorescence staining were further used to measure cell proliferation. The cell clone showed that clone formation was significantly lower in the combined group than in either the DOX or EGCG group, and all of that was lower than the control group (Fig. 1C and D). Immunofluorescence staining showed that Ki-67 protein expressions in the DOX or EGCG group were significantly lower than those in the control group and higher than those in combination (Fig. 1E and F). In short, DOX in synergy with EGCG could significantly induce the proliferation inhibition of 143B cells.

3.2. EGCG in synergy with DOX inhibited osteoclast differentiation and bone resorption

Osteoclasts are commonly induced from BMMs under treatment with recombinant macrophage colony-stimulating factor (M-CSF) and recombinant nuclear factor-κB ligand (RANKL) in vitro (Han, Geng, Liu, Wu, & Wang, 2020). There, we treated the cells during the differentiation of BMMs into osteoclasts with DOX, EGCG, or combination. As shown in Fig. 2A and C, the relative cell size of TRAP-positive multinuclear osteoclast (nuclei > 3) in the combined treatment group was significantly lower than that in the single treatment group, and both

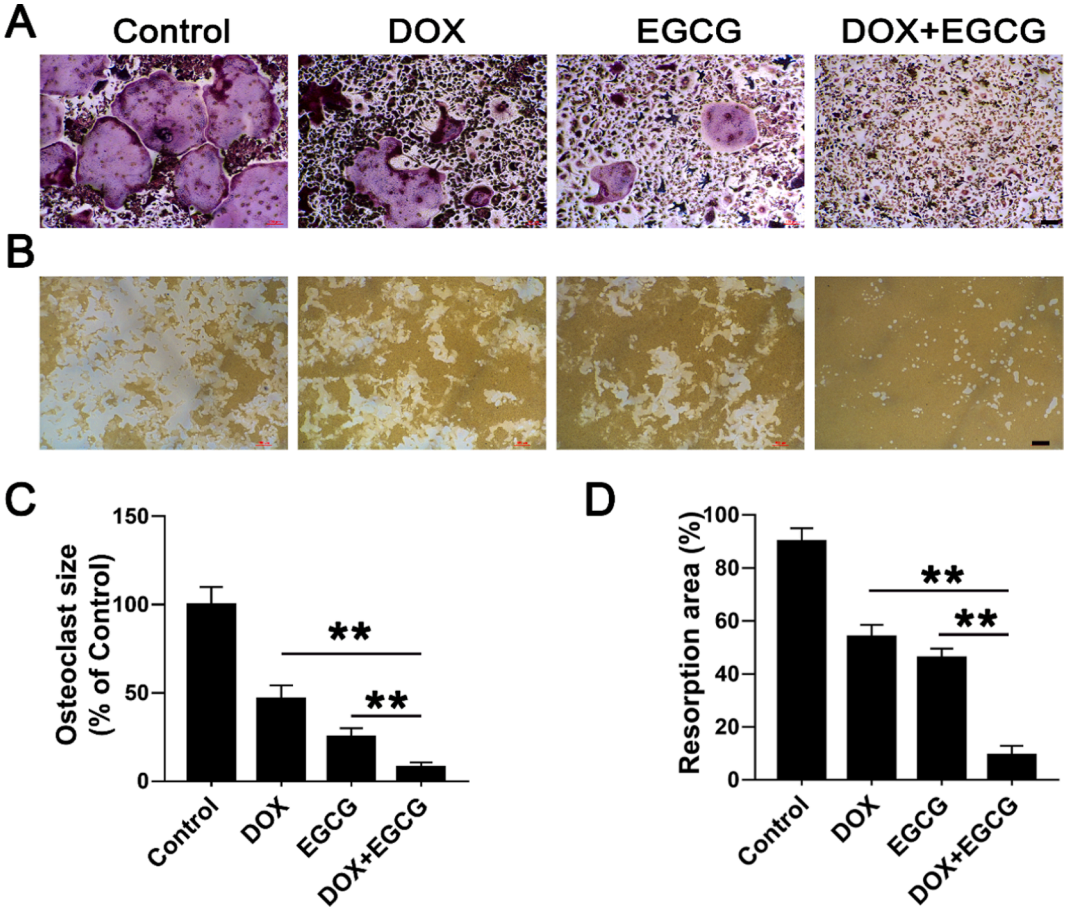

Fig. 2. EGCG in synergy with DOX inhibited RANKL-induced osteoclast formation and bone resorption in vitro. (A) Representative images of TRAP staining showed the osteoclast differentiation of BMMs induced by 50 ng/mL M-CSF and 100 ng/mL RANKL for 4 days. Scale bar = 100 μm. (B) Representative images of resorption pits induced by osteoclasts on Corning Osteoassay 24-well plates. Scale bar = 100 μm. (C) Quantification of TRAP-positive multinuclear cells (nuclei > 3) by relative cell size. (D) Quantification of resorption area using ImageJ software. Data are mean ± SD of triplicate experiments, $^{**}P < 0.01$.

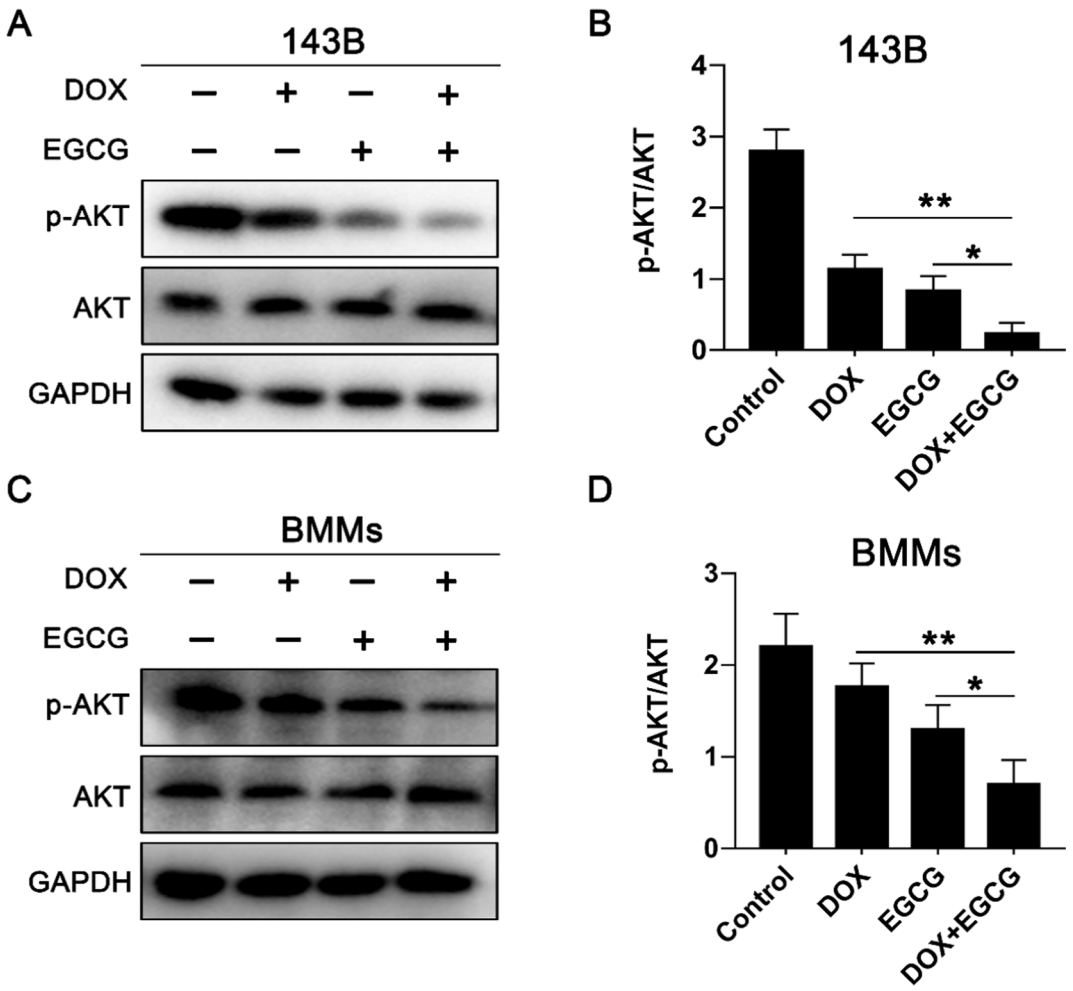

Fig. 3. AKT mediated the synergistic effect of EGCG and DOX. (A) Immunoblot analysis of phosphorylated (p-) and total AKT in treated 143B cells. (B) Quantification of phosphorylated AKT protein expression was normalized to total AKT expression in 143B cells. (C) Immunoblot analysis of phosphorylated (p-) and total AKT in treated BMMs at indicated times. (D) The quantification of phosphorylated AKT protein expression was normalized to total AKT expression in BMMs. Data are mean ± SD for n = 4, *$P < 0.05$, **$P < 0.01$, ***$P < 0.001$.

were lower than the control. Subsequently, we further explored the influence of DOX and EGCG on osteoclastic bone resorption. Consistent with differentiation, the osteoclastic bone resorption in the DOX + EGCG group was less than that in the single treatment group, and both were less than the control. (Fig. 2B and D). Together, these results demonstrated that either DOX or EGCG could inhibit osteoclast formation and bone resorption, but the combination was more effective.

3.3. EGCG in synergy with DOX to attenuate the kinase phosphorylation in 143B cells and BMMs

The phosphorylation of AKT is crucial to the proliferation of osteosarcoma (Zhao et al., 2018). To further explore the mechanism of DOX and EGCG enhancing antitumor, western blot was used to detect AKT phosphorylation after the single or combined action of EGCG and DOX. As shown in Fig. 3A and B, the phosphorylation of AKT in143B cells significantly decreased in DOX or EGCG alone than in the control, and the combined treatment was more significant than the single treatment group. Moreover, RANKL- and M-CSF-induced phosphorylation of AKT is crucial for osteoclastogenesis. DOX or EGCG decreased RANKL- and M-CSF-induced AKT phosphorylation and the combined treatment was more significant than the single treatment group (Fig. 3C and D). Therefore, these results suggested that EGCG + DOX could inhibit AKT phosphorylation by inhibiting cell proliferation and osteoclastogenesis.

3.4. EGCG enhanced DOX-induced tumor inhibition in tibial orthotopic osteosarcoma model mice

We established orthotopic osteosarcoma mouse models to assess the treatment effect of DOX and EGCG in vivo. After intraosseous injection of 143B tumor cells, tumor-bearing nude mice were treated with DOX/DOX + EGCG. As shown in Fig. 4A, rapid tumor growth appeared in the saline-treated group while DOX and EGCG inhibited the tumor growth significantly; tumor growth was markedly slower in the combined treatment group than in the other treatment and control group. There was no significant change in weight (Fig. 4B). After treatment, the tumors in the combined treatment group were significantly smaller visually than those in the single treatment and control (Fig. 4 C and D). Subsequently, hematoxylin and eosin (H&E) staining and Ki-67 staining of the tumor section confirmed that the tumor in the DOX + EGCG group showed less proliferation (Fig. 4E). During the treatment period, no noticeable toxicity was observed in the major organs like the liver, kidney, etc. (Fig. 4F).

3.5. EGCG in synergy with DOX attenuated osteolytic destruction in vivo

Biologically, the osteoclasts and the osteosarcoma cells are mutually reinforced (Mori et al., 2007). Thus, inhibition of osteoclast is a vital way to restrain osteolysis from inhibiting osteosarcoma growth. Three-dimensional reconstruction images of micro-CT showed that the

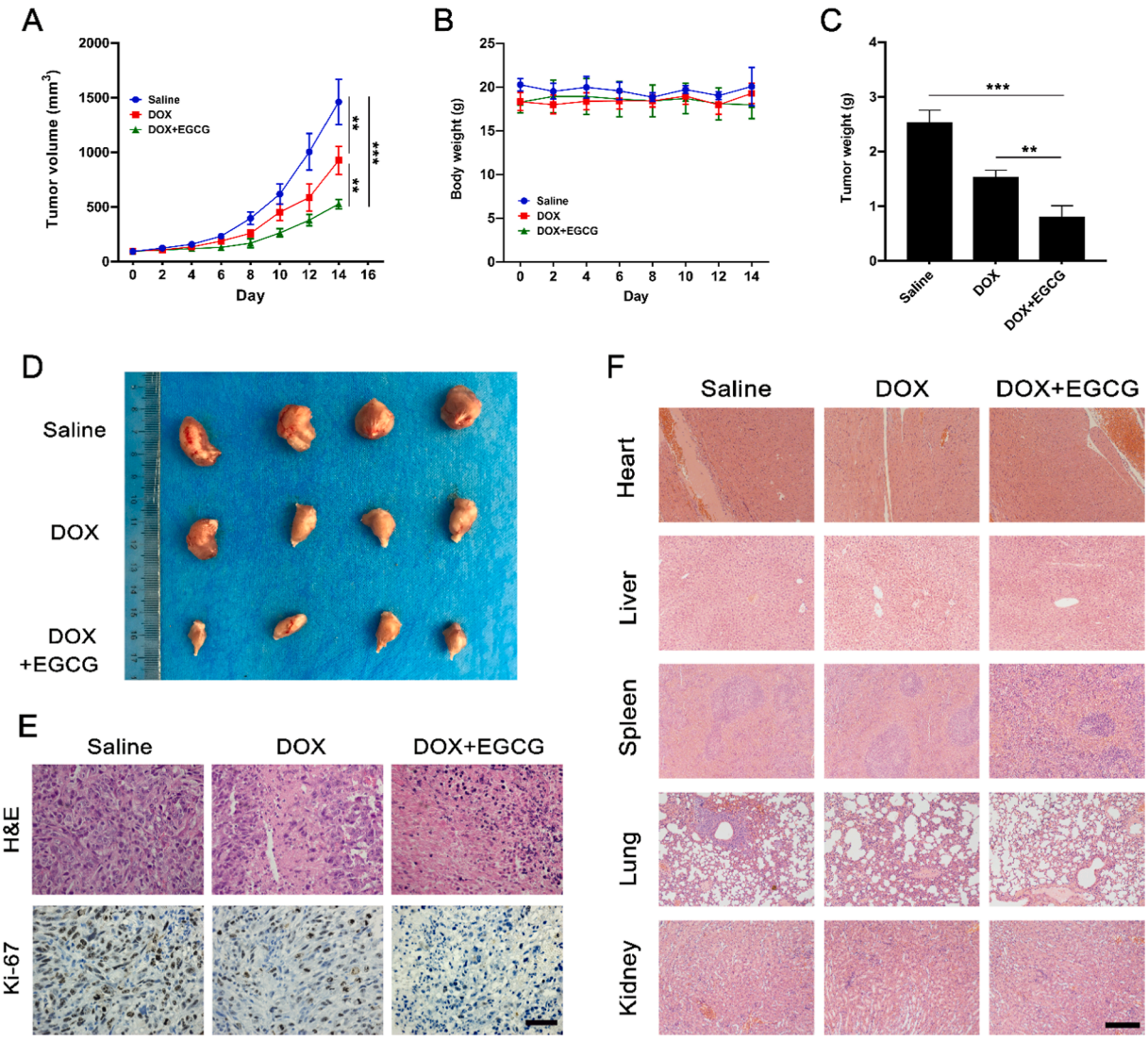

Fig. 4. Antitumor efficacy of EGCG in synergy with DOX in vivo. (A) Tumor growth curve of the 143B cells bearing mice treated as described in different groups (n = 4). (B) Bodyweight of mice in different groups after the indicated treatments for 14 days. n = 4. (C) Tumor weights from each group at the endpoint of the treatment schedule. (D) Representative photographs of the tumor-bearing and normal tibia in different groups after treatment. (E) H&E and Ki-67 staining images of the tumors from each group, respectively. Scale bar = 50 μm. (F) H&E staining images of the major organs from each group, respectively. Scale bar = 200 μm. Data are mean ± SD for n = 4, *$P < 0.05$, **$P < 0.01$, ***$P < 0.001$.

combined treatment with EGCG and DOX resulted in significantly lower bone tissue destruction than that of the group treated with DOX alone or saline (Fig. 5A-F). TRAP staining further confirmed the osteoclast level at the site of the osteolytic lesion. As shown in Fig. 5G, the TRAP staining-positive cells were significantly reduced, indicating that osteoclasts in the osteolytic site were inhibited after EGCG + DOX treatment.

4. Discussion

Osteosarcoma, with extremely high nausea, is the most common primary bone cancer in children and young adults and most commonly arises in the metaphysis of the long bones near the growth plates (Kansara et al., 2019). Clinically, surgical excision and adjuvant chemotherapy, long-term survival in >60% of patients presenting with localized disease (Isakoff, Bielack, Meltzer, & Gorlick, 2015). However, limited therapeutic progress has been made over the past four decades. Multidrug combined chemotherapy is one of the essential methods in treating osteosarcomas, such as cisplatin, methotrexate and Adriamycin (Isakoff, Bielack, Meltzer, & Gorlick, 2015). However, the application of these drugs can lead to drug resistance and bone loss, which undermine the efficacy of these drugs in treating osteosarcoma (Xiao et al., 2018). Therefore, an innovative additional adjuvant therapeutic strategy is needed to enhance the therapeutic effect of osteosarcoma patients.

Osteoclasts are the essential cells for the progression of osteosarcoma. Osteosarcoma secretes osteoclast-stimulating cytokines that promote bone resorption, while tumor growth is stimulated by factors released during osteolysis. Osteoclast targeted therapy is a potential treatment for osteosarcoma. For example, Heymann. *et al.* proved that zoledronic acid combined with ifosfamide enhances tumor regression and tissue repair in rat osteosarcoma (Heymann et al., 2005). Geng. *et al.* demonstrated that the application of nanomedicine combined with inhibiting cancer cell growth and inhibiting the activity of osteoclasts could inhibit the growth of osteosarcoma (Geng et al., 2021). Therefore, inhibiting cancer cell growth and inhibiting the activity of osteoclasts are two primary strategies to treat osteosarcoma.

Many natural plants have antitumor active ingredients (Nani et al., 2019; Zhang et al., 2020). As a natural plant, tea contains a variety of anti-tumor components, such as flavonoids, which can inhibit the growth of osteosarcoma through multiple mechanisms (Shi et al., 2021). EGCG, the major catechin in green tea, has been reported to promote the

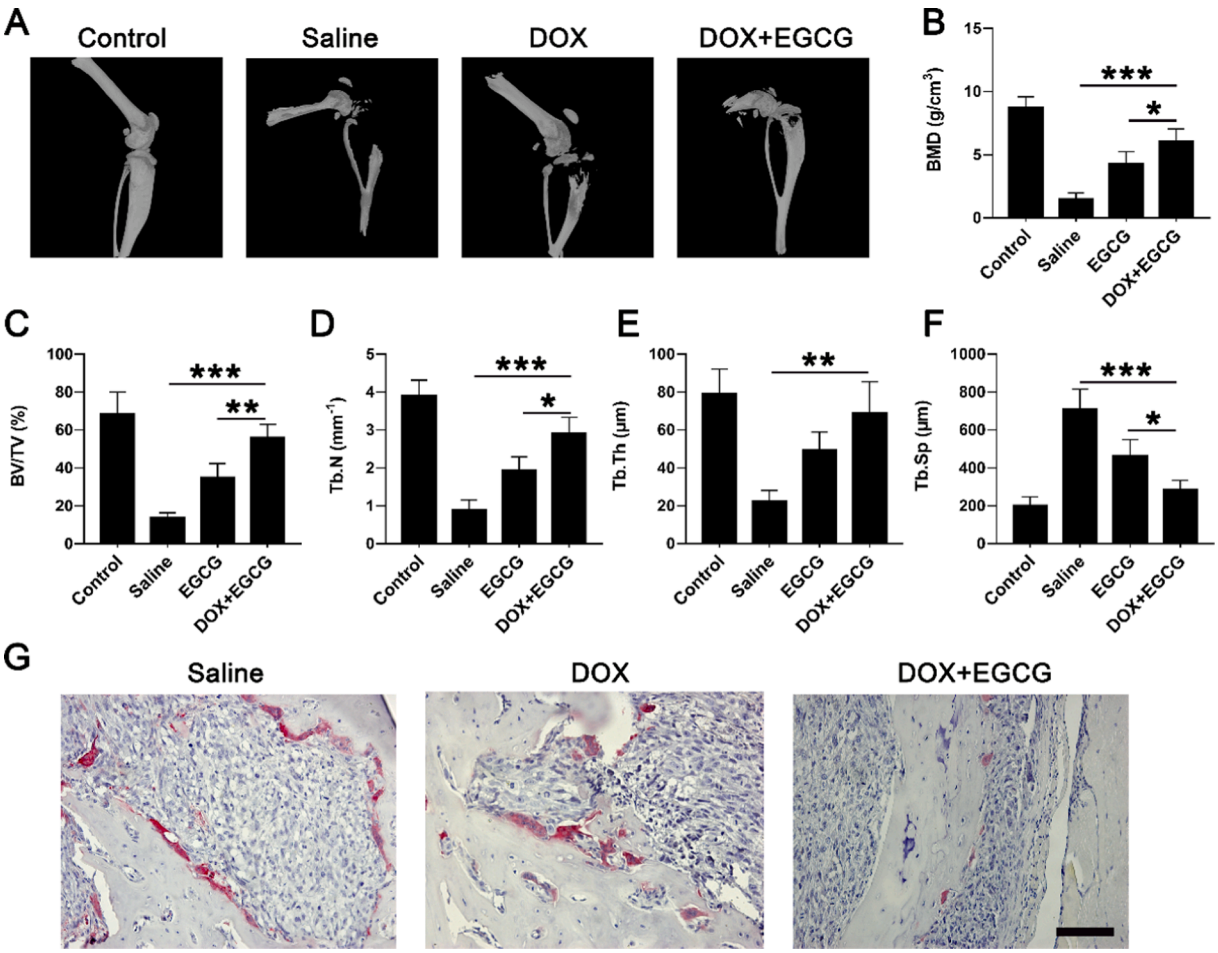

Fig. 5. DOX in synergy with EGCG attenuated the 143B cells induced osteolysis in vivo. (A) Representative images of micro-CT for tumor-bearing tibia or healthy tibia in mice in each group. (B-F) Quantitative micro-CT analysis of BMD (B), BV/TV (C), Tb.N (D), Tb.Th (E) and Tb.Sp (F). (G) Bone histological examination of the tumor-bearing tibia using TRAP staining in each group. Data are mean ± SD; *$P < 0.05$; **$P < 0.01$; ***$P < 0.001$.

sensitivity of traditional chemotherapy drugs and reverse multidrug resistance (Esmaeili, 2016; P. Wang, Henning, Heber, & Vadgama, 2015; Wang, Pan, Chen, Guo, & Wang, 2021). Similarly, EGCG was shown to exert a significant inhibitory effect on the proliferation and invasion of osteosarcoma cells (Zhu & Wang, 2016). Chaoqun Dong *et al.* indicated that EGCG inhibited osteosarcoma growth by regulating the Wnt/β-catenin pathway and that EGCG can be used alone or in combination with other regimens as a potentially effective anticancer treatment (Dong et al., 2022). Guoqing Tang *et al.* demonstrated that EGCG could inhibit the metastasis capability of osteosarcoma cells by inhibiting MEK/ERK signaling activity (Tang et al., 2015). However, the understanding of EGCG's combined effect and mechanism with commonly used chemotherapy drugs is still unclear. In this study, DOX alone or in combination with EGCG could reduce the proliferation of osteosarcoma cells, but the combined effect was more obvious (Fig. 1). Moreover, EGCG in synergy with DOX inhibited osteoclast differentiation and bone resorption. The phosphorylation of AKT is crucial to the proliferation of osteosarcoma and osteoclastogenesis (Amarasekara et al., 2018; Zhao et al., 2018). To further explore the mechanism of DOX and EGCG enhancing antitumor and anti-osteoclastogenesis, western blot was used to detect AKT phosphorylation after the single or combined action of EGCG and DOX. The phosphorylation of AKT in143B cells and BMMs have significantly decreased in DOX or EGCG alone than in the control, and the combined treatment was more significant than the single treatment group (Fig. 3A-C). These results indicated that EGCG in synergy with DOX exerted biological effects that appear to act in part through the AKT phosphorylation.

Considering the effects on DOX and EGCG enhancing 143B cells proliferation inhibition and osteoclastogenesis inhibition in vitro, we then established orthotopic osteosarcoma mouse models to assess the effect in vivo. Tumor growth was significantly slower in DOX and EGCG combination treatment group than in the other treatment and control group (Fig. 4A). These results confirmed that EGCG in synergy with DOX attenuated tumor growth in vivo. Biologically, the osteoclasts and the osteosarcoma microenvironment synergistically regulate one another to create a "vicious circle" that favors osteolysis and tumor expansion (Mori et al., 2007). Osteoclast targeted therapy is a potential treatment for osteosarcoma. Three-dimensional reconstruction images of micro-CT showed that the combined treatment with EGCG and DOX resulted in significantly lower bone tissue destruction than that of the group treated with DOX alone or saline (Fig. 5A-F). The TRAP staining-positive cells were significantly reduced, indicating that osteoclasts in the osteolytic site were inhibited after EGCG + DOX treatment. In short, EGCG could inhibit osteoclastogenesis at the tumor-bone interface to restrain osteolysis.

5. Conclusion

In summary, these data demonstrated that EGCG could enhance the anti-osteosarcoma effect of DOX in vivo and in vitro. Moreover, the combination of DOX and EGCG could inhibit the activity of osteoclasts at the tumor-bone interface, thereby preventing tumor-induced osteolysis and blocking the vicious circle. Taken together, EGCG may be used as an adjuvant chemotherapy drug to treat osteosarcoma.

CRediT authorship contribution statement

Dongcai Hu: Methodology, Validation, Investigation, Writing – original draft, Writing – review & editing. **KeJiang Lin:** Investigation, Writing – review & editing. **Xiang Gao:** Funding acquisition, Writing – review & editing. **Mengxue Zhou:** Conceptualization, Validation, Writing – review & editing, Supervision. **Huan Geng:** Conceptualization, Methodology, Validation, Investigation, Resources, Data curation, Writing – original draft, Writing – review & editing, Supervision, Project administration.

Declaration of Competing Interest

The authors declare that they have no known competing financial interests or personal relationships that could have appeared to influence the work reported in this paper.

Acknowledgments

This work was supported by grants from Natural Science Foundation of Zhejiang Province (Y21H070011).

Ethical statement

All animal care was approved by the Animal Welfare Committee in Zhejiang University School of Medicine (Permit Number: 2020-0011).

References

Amarasekara, D. S., Yun, H., Kim, S., Lee, N., Kim, H., & Rho, J. (2018). Regulation of osteoclast differentiation by cytokine networks. *Immune Network, 18*(1), e8.

Baa, A. K., & Rastogi, S. (2021). Combination doxorubicin and pembrolizumab in patients with advanced Anthracycline-Naive Sarcoma. *JAMA Oncology, 7*(3), 465.

Chen, Y., Di Grappa, M. A., Molyneux, S. D., McKee, T. D., Waterhouse, P., Penninger, J. M., & Khokha, R. (2015). RANKL blockade prevents and treats aggressive osteosarcomas. *Science Translational Medicine, 7*(317), 317ra197.

Dong, C., Wang, Z., Shen, P., Chen, Y., Wang, J., & Wang, H. (2022). Epigallocatechin-3-gallate suppresses the growth of human osteosarcoma by inhibiting the Wnt/β-catenin signalling pathway. *Bioengineered, 13*(4), 8490–8502.

Du, C., Zhou, M., Jia, F., Ruan, L., Lu, H., Zhang, J., … Hu, Y. (2021). D-arginine-loaded metal-organic frameworks nanoparticles sensitize osteosarcoma to radiotherapy. *Biomaterials, 269*, 120642.

Esmaeili, M. A. (2016). Combination of siRNA-directed gene silencing with epigallocatechin-3-gallate (EGCG) reverses drug resistance in human breast cancer cells. *Journal of Chemical Biology, 9*(1), 41–52.

Gan, R. Y., Li, H. B., Sui, Z. Q., & Corke, H. (2018). Absorption, metabolism, anti-cancer effect and molecular targets of epigallocatechin gallate (EGCG): An updated review. *Critical Reviews in Food Science and Nutrition, 58*(6), 924–941.

Geng, H., Chang, Y. N., Bai, X., Liu, S., Yuan, Q., Gu, W., … Xing, G. (2017). Fullerenol nanoparticles suppress RANKL-induced osteoclastogenesis by inhibiting differentiation and maturation. *Nanoscale, 9*(34), 12516–12523.

Geng, H., Zhou, M., Li, B., Liu, L., Yang, X., Wen, Y., … Chen, L. (2021). Metal-drug nanoparticles-mediated osteolytic microenvironment regulation for enhanced radiotherapy of orthotopic osteosarcoma. *Chemical Engineering Journal, 417*, 128103.

Gill, J., & Gorlick, R. (2021). Advancing therapy for osteosarcoma. *Nature Reviews Clinical Oncology, 18*(10), 609–624.

Han, B., Geng, H., Liu, L., Wu, Z., & Wang, Y. (2020). GSH attenuates RANKL-induced osteoclast formation in vitro and LPS-induced bone loss in vivo. *Biomedicine & Pharmacotherapy, 128*, 110305.

Heymann, D., Ory, B., Blanchard, F., Heymann, M. F., Coipeau, P., Charrier, C., … Redini, F. (2005). Enhanced tumor regression and tissue repair when zoledronic acid is combined with ifosfamide in rat osteosarcoma. *Bone, 37*(1), 74–86.

Isakoff, M. S., Bielack, S. S., Meltzer, P., & Gorlick, R. (2015). Osteosarcoma: Current treatment and a collaborative pathway to success. *Journal of Clinical Oncology, 33*(27), 3029–3035.

Kansara, M., Thomson, K., Pang, P., Dutour, A., Mirabello, L., Acher, F., … Thomas, D. M. (2019). Infiltrating myeloid cells drive osteosarcoma progression via GRM4 regulation of IL23. *Cancer Discovery, 9*(11), 1511–1519.

Labrinidis, A., Hay, S., Liapis, V., Ponomarev, V., Findlay, D. M., & Evdokiou, A. (2009). Zoledronic acid inhibits both the osteolytic and osteoblastic components of osteosarcoma lesions in a mouse model. *Clinical Cancer Research, 15*(10), 3451–3461.

Lee, J. A., Jung, J. S., Kim, D. H., Lim, J. S., Kim, M. S., Kong, C. B., … Koh, J. S. (2011). RANKL expression is related to treatment outcome of patients with localized, high-grade osteosarcoma. *Pediatric Blood & Cancer, 56*(5), 738–743.

Liu, L., Geng, H., Mei, C., & Chen, L. (2021). Zoledronic acid enhanced the antitumor effect of cisplatin on orthotopic osteosarcoma by ROS-PI3K/AKT signaling and attenuated osteolysis. *Oxidative Medicine and Cellular Longevity, 2021*, 6661534.

Mori, K., Le Goff, B., Berreur, M., Riet, A., Moreau, A., Blanchard, F., … Heymann, D. (2007). Human osteosarcoma cells express functional receptor activator of nuclear factor-kappa B. *The Journal of Pathology, 211*(5), 555–562.

Nani, A., Belarbi, M., Murtaza, B., Benammar, C., Merghoub, T., Rialland, M., … Hichami, A. (2019). Polyphenols from Pennisetum glaucum grains induce MAP kinase phosphorylation and cell cycle arrest in human osteosarcoma cells. *Journal of Functional Foods, 54*, 422–432.

Ren, W., Cai, X., Chen, J., Ruan, L., Lu, H., Zhang, J., … Gao, J. (2021). GM-CSF-loaded nanoparticles for photothermal-assisted immunotherapy against orthotopic bladder cancer. *Oncologie, 23*(3), 359–371.

Ruan, L., Chen, J., Du, C., Lu, H., Zhang, J., Cai, X., … Hu, Y. (2022). Mitochondrial temperature-responsive drug delivery reverses drug resistance in lung cancer. *Bioactive Materials, 13*, 191–199.

Shi, J., Yang, G., You, Q., Sun, S., Chen, R., Lin, Z., … Lv, H. (2021). Updates on the chemistry, processing characteristics, and utilization of tea flavonoids in last two decades (2001–2021). *Critical Reviews in Food Science and Nutrition*, 1–28.

Tang, G., Zhang, Z., Qian, H., Chen, J., Wang, Y., Chen, X., … Chen, Y. (2015). (-)-Epigallocatechin-3-gallate inhibits osteosarcoma cell invasiveness by inhibiting the MEK/ERK signaling pathway in human osteosarcoma cells. *Journal of Environmental Pathology, Toxicology and Oncology, 34*(1), 85–93.

Wang, P., Henning, S. M., Heber, D., & Vadgama, J. V. (2015). Sensitization to docetaxel in prostate cancer cells by green tea and quercetin. *Journal of Nutritional Biochemistry, 26*(4), 408–415.

Wang, W., Chen, D., & Zhu, K. (2018). SOX2OT variant 7 contributes to the synergistic interaction between EGCG and Doxorubicin to kill osteosarcoma via autophagy and stemness inhibition. *Journal of Experimental & Clinical Cancer Research, 37*(1), 37.

Wang, Y., Pan, H., Chen, D., Guo, D., & Wang, X. (2021). Targeting at cancer energy metabolism and lipid droplet formation as new treatment strategies for epigallocatechin-3-gallate (EGCG) in colorectal cancer cells. *Journal of Functional Foods, 83*.

Xiao, X., Wang, W., Li, Y., Yang, D., Li, X., Shen, C., … Guo, Z. (2018). HSP90AA1-mediated autophagy promotes drug resistance in osteosarcoma. *Journal of Experimental & Clinical Cancer Research, 37*(1), 201.

Xu, H., Liu, T., Jia, Y., Li, J., Jiang, L., Hu, C., … Sheng, J. (2021). (-)-Epigallocatechin-3-gallate inhibits osteoclastogenesis by blocking RANKL-RANK interaction and suppressing NF-κB and MAPK signaling pathways. *International Immunopharmacology, 95*, 107464.

Xu, H., Liu, T., Li, J., Xu, J., Chen, F., Hu, L., … Sheng, J. (2019). Oxidation derivative of (-)-epigallocatechin-3-gallate (EGCG) inhibits RANKL-induced osteoclastogenesis by suppressing RANK signaling pathways in RAW 264.7 cells. *Biomedicine & Pharmacotherapy, 118*, 109237.

Zhang, X., Duan, S., Tao, S., Huang, J., Liu, C., Xing, S., … Wei, G. (2020). Polysaccharides from Dendrobium officinale inhibit proliferation of osteosarcoma cells and enhance cisplatin-induced apoptosis. *Journal of Functional Foods, 73*, 104143.

Zhao, G. S., Gao, Z. R., Zhang, Q., Tang, X. F., Lv, Y. F., Zhang, Z. S., … Guo, Q. N. (2018). TSSC3 promotes autophagy via inactivating the Src-mediated PI3K/Akt/mTOR pathway to suppress tumorigenesis and metastasis in osteosarcoma, and predicts a favorable prognosis. *Journal of Experimental & Clinical Cancer Research, 37*(1), 188.

Zhou, M., Huang, H., Wang, D., Lu, H., Chen, J., Chai, Z., … Hu, Y. (2019). Light-triggered PEGylation/dePEGylation of the nanocarriers for enhanced tumor penetration. *Nano Letters, 19*(6), 3671–3675.

Zhu, K., & Wang, W. (2016). Green tea polyphenol EGCG suppresses osteosarcoma cell growth through upregulating miR-1. *Tumor Biology, 37*(4), 4373–4382.